



Colloidal State of Exfoliated Oxide Nanosheets of Layered Niobate Characterized with a Molecular-Level Spectroscopic Technique and Macroscopic Observations

Teruyuki Nakato* and Jun Sugawara

Division of Bio-Applications and Systems Engineering (BASE), Institute of Symbiotic Science and Technology, Tokyo University of Agriculture and Technology, 2-24-16 Naka-cho, Koganei, Tokyo 184-8588

Received May 16, 2007; E-mail: tnakat@cc.tuat.ac.jp

Inorganic oxide nanosheets, prepared by exfoliation of layered hexaniobate $\text{K}_4\text{Nb}_6\text{O}_{17}$, were investigated in a colloidal state with different hierarchies: micrometer to submillimeter level with microscopies and molecular level with visible spectroscopy. A cationic porphyrin 5,10,15,20-tetrakis(*N*-methylpyridinium-4-yl)-21*H*,23*H*-porphine (H_2TMPyP) was added to the colloid as a spectroscopic probe. The Soret absorption band of porphyrin adsorbed on the niobate nanosheets was split when the colloid was concentrated. The modified spectral profile was retained when the colloid was re-diluted, indicating irreversible alteration that reflected concentration history of the dispersed state of the nanosheets. Fluorescence optical and transmission electron microscopies indicated aggregation and crumpling of the nanosheets in the colloids that were concentrated. The alteration of the colloidal nanosheets upon concentration was ascribed to the enrichment of electrolytes coexisting in the colloid. The results demonstrated that the microscopic status of the colloiddally dispersed exfoliated nanosheets is related to the microenvironments formed by functional molecules immobilized on the nanosheets.

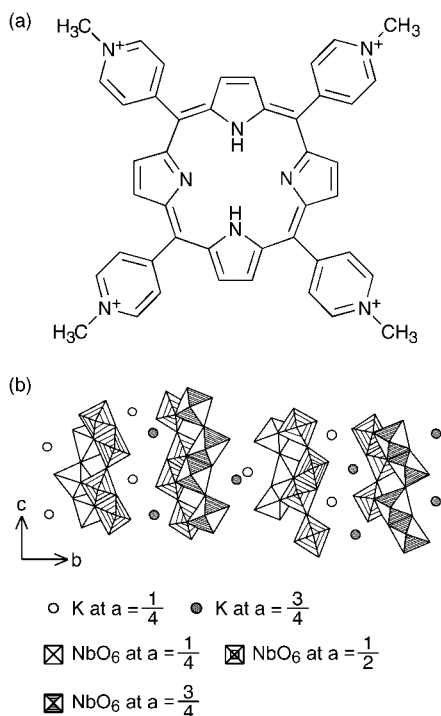
Exfoliation of inorganic layered materials has attracted great attention in the past decade.^{1,2} Exfoliated single inorganic layers, called nanosheets, are highly anisotropic particles having a thickness of around 1 nm and a lateral dimension of more than 1 μm . Whereas many layered compounds have been found to form nanosheets through exfoliation, layered niobates and titanates have been recognized as an important class of materials because of their photocatalytic activities.³ In fact, exfoliation behavior has been investigated for various layered niobates and titanates, such as $\text{HCa}_2\text{-Nb}_3\text{O}_{10}$,^{4,5} $\text{K}_4\text{Nb}_6\text{O}_{17}$,^{2,6} $\text{H}_{0.7}\text{Ti}_{1.8}\text{O}_4$,⁷ HTiNbO_5 ,^{5,8} $\text{H}_2\text{Ti}_4\text{O}_9$,⁹ and HNb_3O_8 .¹⁰

Exfoliated nanosheets are usually obtained as colloids, which can exhibit peculiar properties. They bear electrical charges in most cases (e.g., the niobate and titanate layers are negatively charged), and their colloids, which are called “nanosheet colloids” hereafter, are metastable in a thermodynamic sense. Thus, the dispersed state of nanosheets can be altered by subtle differences in the conditions of the colloids, and the alteration can occur often irreversibly even during routine handling of the colloids, such as concentration, dilution, and addition of ionic species. For example, electrolytes coexisting in the colloids may induce morphological modification and (partial) aggregation of the nanosheets. However, colloidal properties of the exfoliated inorganic nanosheets have not been investigated systematically until this century except for clay minerals.¹¹

The colloidal state of exfoliated nanosheets is important not only for fundamental knowledge but also for applying the nanosheets to solid nanomaterials^{8,12} through controlled reassembling from colloidal states, although most of the studies

have recognized the nanosheets only as building blocks. The colloidal state can be detected at both microscopic and macroscopic levels. For probing at molecular level, we can utilize spectroscopic behavior of dyes adsorbed on the nanosheets, since the dispersed state of the nanosheets is reflected by the microenvironments around the dyes. Nevertheless, spectroscopic properties of dyes in nanosheet colloids have scarcely been investigated in relation to the colloidal state of nanosheets.

We attempted in the present study to observe the changes in the colloiddally dispersed state of inorganic nanosheets prepared by exfoliation of layered hexaniobate $\text{K}_4\text{Nb}_6\text{O}_{17}$ at the molecular level via the spectroscopic behavior of a dye as well as at macroscopic level with microscope techniques. We used a cationic porphyrin, 5,10,15,20-tetrakis(*N*-methylpyridinium-4-yl)-21*H*,23*H*-porphine (H_2TMPyP), adsorbed on negatively charged niobate nanosheets as a probe dye. Figure 1 shows the structure of H_2TMPyP and $\text{K}_4\text{Nb}_6\text{O}_{17}$. Porphyrins are invaluable functional dyes because they have the capability for photoenergy conversion.^{13,14} Spectroscopic investigations of porphyrins adsorbed on inorganic layered materials have been carried out for both aqueous suspensions and solid intercalation compounds.^{15–17} We found in the present study that the spectroscopic behavior of the porphyrin irreversibly changed when the nanosheet colloid was concentrated. The results demonstrate linkage of the spectroscopic behavior at molecular level to an alteration of the dispersed state of nanosheets at micrometer to submillimeter level. To our knowledge, it is the first time that changes in nanosheet colloids extending over different structural hierarchies has been observed.

Fig. 1. Structure of (a) H_2TMPyP and (b) $\text{K}_4\text{Nb}_6\text{O}_{17}$.

Experimental

Preparation of the Starting Niobate Nanosheet Colloid.

The niobate nanosheets were prepared by exfoliation of tetrapotassium hexaniobate $\text{K}_4\text{Nb}_6\text{O}_{17}$ according to the method reported previously.^{18,19} Briefly, single crystalline $\text{K}_4\text{Nb}_6\text{O}_{17}$ ²⁰ prepared by a flux method was allowed to react with an aqueous solution of propylammonium hydrochloride. This treatment displaced K^+ ions located between the $\text{Nb}_6\text{O}_{17}^{4-}$ layers for propylammonium ions to exfoliate the layers. The exfoliated material was recovered by centrifugation, and the deposit obtained was washed by stirring in water for 15 min. After repeating the washing twice, the colloid was subjected to centrifugation and re-dispersed in water to yield a colloid containing ca. $1 \times 10^{-2} \text{ mol dm}^{-3}$ of $\text{Nb}_6\text{O}_{17}^{4-}$ nanosheets. This sample was diluted with a $3 \times 10^{-5} \text{ mol dm}^{-3}$ aqueous solution of H_2TMPyP *p*-toluenesulfonate (Wako Pure Chemical Ind., used as received) and then with water. This sample, named sample **1**, was used as the starting nanosheet colloid. The nanosheet content was set to $[\text{Nb}_6\text{O}_{17}^{4-}] = 2.5 \times 10^{-3} \text{ mol dm}^{-3}$, and

the amount of H_2TMPyP was adjusted to a $\text{H}_2\text{TMPyP}/\text{Nb}_6\text{O}_{17}^{4-}$ molar ratio of $\approx 5 \times 10^{-3}$.

Treatment of the Nanosheet Colloid. The colloid was subjected to various treatments to yield samples **2–6**. Table 1 summarizes the samples prepared in the present study. The starting colloid (sample **1**) was concentrated up to $[\text{Nb}_6\text{O}_{17}^{4-}] = 4.8 \times 10^{-2}$ and $1.8 \times 10^{-1} \text{ mol dm}^{-3}$ by heating at 353 K to yield samples **2a** and **3a**, respectively. Then, samples **2a** and **3a** were re-diluted to the initial nanosheet content ($[\text{Nb}_6\text{O}_{17}^{4-}] = 2.5 \times 10^{-3}$) to yield samples **2b** and **3b**, respectively. The $\text{H}_2\text{TMPyP}/\text{Nb}_6\text{O}_{17}^{4-}$ ratio was maintained during these treatments. Sample **4** was prepared by adding H_2TMPyP after concentrating a dilute colloid. A nanosheet colloid excluding the porphyrin with $[\text{Nb}_6\text{O}_{17}^{4-}] = 2.5 \times 10^{-3} \text{ mol dm}^{-3}$ (the same as the nanosheet content of sample **1**) was concentrated to $[\text{Nb}_6\text{O}_{17}^{4-}] = 2.8 \times 10^{-1} \text{ mol dm}^{-3}$. H_2TMPyP was added to this concentrated sample, and then, the colloid was re-diluted to the initial nanosheet content to yield sample **4**. The amount of H_2TMPyP added was the same as those of the other samples (molar ratio of $\text{H}_2\text{TMPyP}/\text{Nb}_6\text{O}_{17}^{4-} \approx 5 \times 10^{-3}$). Sample **5** was obtained not by concentrating the colloid, but by adding an aqueous KCl solution (0.1 mol dm^{-3}) to sample **1** in order to examine the influence of co-existing electrolytes. The amount of KCl added in the colloid was $1.2 \times 10^{-3} \text{ mol dm}^{-3}$.

Instruments. Transmission electron microscope (TEM) images of the samples were taken on a Hitachi H-7100 microscope. A small portion of nanosheet colloid was added to a mixture of water and methanol, and loaded on a grid coated with a collodion membrane followed by drying at 333 K. Visible spectra of the colloid samples were recorded on a Shimadzu UV-2450 spectrophotometer by using a transmission method. Fluorescence microscope observations were carried out with an Olympus BX51 optical microscope equipped with a BX2-FL-1 fluorescence system and a U-MSWB2 mirror unit, by which the Soret absorption of porphyrin was excited. Fluorescence spectra were measured on a Jasco FP-6500 spectrofluorometer.

Results

Characterization of the Niobate Nanosheet Colloid Containing H_2TMPyP .

The niobate nanosheet colloid containing a small amount of H_2TMPyP shows almost the same properties at the macroscopic level as those of the nanosheet colloid without H_2TMPyP . The starting colloid (sample **1**) exhibited liquid crystallinity as evidenced with birefringence, as indicated by the photograph of the colloid placed between crossed

Table 1. Colloid Samples Prepared in the Present Study

Sample	Nanosheet content / $\text{mol-Nb}_6\text{O}_{17}^{4-} \text{ dm}^{-3}$	Preparation procedure
1	2.5×10^{-3}	Starting unconcentrated colloid including H_2TMPyP ($\text{H}_2\text{TMPyP}/\text{Nb}_6\text{O}_{17} \approx 5 \times 10^{-3}$)
2a	4.8×10^{-2}	Concentration of 1
2b	2.5×10^{-3}	Re-dilution of 2a with water
3a	1.8×10^{-1}	Concentration of 1
3b	2.5×10^{-3}	Re-dilution of 3a with water
4	2.5×10^{-3}	Concentrating a dilute colloid of $2.5 \times 10^{-3} \text{ mol-Nb}_6\text{O}_{17}^{4-} \text{ dm}^{-3}$ excluding H_2TMPyP to $2.8 \times 10^{-1} \text{ mol-Nb}_6\text{O}_{17}^{4-} \text{ dm}^{-3}$, adding H_2TMPyP ($\text{H}_2\text{TMPyP}/\text{Nb}_6\text{O}_{17} \approx 5 \times 10^{-3}$), and then re-diluting
5	2.5×10^{-3}	Adding KCl to 1 up to $1.2 \times 10^{-3} \text{ mol dm}^{-3}$

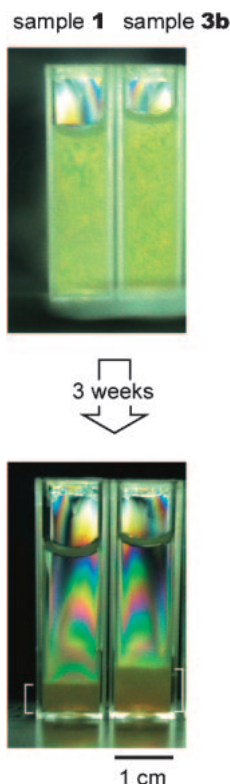


Fig. 2. Photographs of samples **1** (starting unconcentrated nanosheet colloid) and **3b** (highly concentrated and re-diluted colloid) in quartz cuvettes between crossed polarizers. Upper and lower images indicate the samples 3 min and 3 weeks after poured into the cuvettes, respectively. The samples 3 min after pouring show birefringence due to liquid crystallinity (upper image) while settled nanosheets are observed in the samples after 3 weeks (lower image).

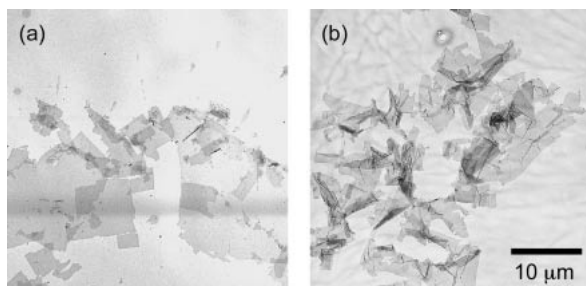


Fig. 3. TEM images of the niobate nanosheets recovered from (a) sample **1** (starting unconcentrated nanosheet colloid) and (b) sample **3a** (concentrated nanosheet colloid).

polarizers shown in Fig. 2. This behavior is the same as that observed for the niobate nanosheet colloids without H_2TMPyP ,^{18,21} which is attributed to high anisotropy of the nanosheets.²² TEM image of the nanosheets recovered from the sample exhibited thin platelets, as shown in Fig. 3a, which is similar to that observed for the colloids without H_2TMPyP .¹⁸

On the other hand, H_2TMPyP in sample **1** gives a visible absorption spectrum similar to that of an aqueous H_2TMPyP solution. Figures 4a and 4b compare the absorption spectra

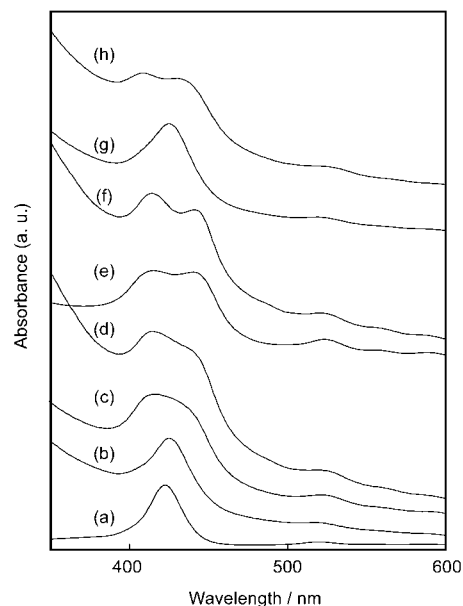


Fig. 4. Visible absorption spectra of (a) H_2TMPyP aqueous solution ($1.3 \times 10^{-5} \text{ mol dm}^{-3}$), (b) sample **1** (starting unconcentrated nanosheet colloid), (c) sample **2a** (moderately concentrated nanosheet colloid), (d) sample **2b** (re-diluted sample **2a**), (e) sample **3a** (highly concentrated nanosheet colloid), (f) sample **3b** (re-diluted sample **3a**), (g) sample **4** (nanosheet colloid where H_2TMPyP was added after concentration), and (h) sample **5** (electrolyte-added nanosheet colloid).

of H_2TMPyP in an aqueous solution and in the colloid sample. The Soret absorption band of the porphyrin in the colloid appeared at 425 nm, which is slightly red-shifted from the absorption at 422 nm observed in the aqueous solution. We confirmed that the amount of H_2TMPyP distributed in the supernatant after centrifugation of sample **1** was less than 1% of the porphyrin molecules initially added to the colloid. Hence, H_2TMPyP molecules contained in the colloid are almost all adsorbed on the niobate nanosheets, and the adsorption does not significantly modify the spectrum of H_2TMPyP . If the adsorbed H_2TMPyP molecules are homogeneously distributed on the niobate nanosheets, the surface area of the nanosheet occupied by a porphyrin molecule is estimated to be 97 nm^2 .²³ This area means that the average distance between adjacent H_2TMPyP molecules is 9.8 nm; the distance is much larger than the molecular size of an H_2TMPyP molecule (1.64 nm, estimated as distance between two diagonal cationic sites¹⁷).

Spectroscopic Behavior of H_2TMPyP Reflecting the Concentration History of the Colloid. The spectral profile of H_2TMPyP adsorbed on the niobate nanosheets changed when the colloid was concentrated. Figures 4c and 4e show the spectra of samples **2a** and **3a**, which were obtained by concentrating sample **1**. The Soret bands were broadened in the moderately concentrated colloid (sample **2a**) and split in the highly concentrated one (sample **3a**).

The spectral changes irreversibly occurred due to the concentration treatment. The modified Soret band of H_2TMPyP in the concentrated colloids remained when they were re-diluted to the initial nanosheet content ($[\text{Nb}_6\text{O}_{17}^{4-}] = 2.5 \times 10^{-3} \text{ mol dm}^{-3}$). Figures 4d and 4f give the absorption spectra

of samples **2b** and **3b**, which are obtained by re-diluting samples **2a** and **3a**, respectively. The spectroscopic features (broadening or splitting of the Soret band) observed for the concentrated samples were also observed for the re-diluted samples. These facts mean that the microenvironments around H_2TMPyP molecules are irreversibly modified by concentrating the nanosheet colloids depending on the degree of concentration; the concentration history is “memorized” in the re-diluted colloids. However, the apparent dispersed state of the colloid remains after the concentration–dilution cycle, which is represented by liquid crystallinity of sample **3b** observed similarly to sample **1** as shown in Fig. 2.

The change in the porphyrin spectra occurred only when the niobate nanosheets were concentrated together with the probe molecules. Figure 4g shows the absorption spectrum of sample **4**, to which H_2TMPyP was added after concentrating the nanosheet colloid. Although the sample was prepared through concentration and re-dilution, the spectrum characterized by a single Soret band at 426 nm without broadening is the same as that of the unconcentrated sample **1**. This result suggests that the niobate nanosheets form closed internal microvoids upon concentration and that the microvoids are not accessible to H_2TMPyP molecules after their formation.

Morphological Modification of the Nanosheets upon Concentration. Fluorescence microscope observations showed the modification of the dispersed state of nanosheets upon concentration. Figure 5 compares typical fluorescence microscope images of the nanosheet colloid obtained by exciting the Soret band before and after concentration. The image of unconcentrated sample **1**, which shows red fluorescence spreading over the entire view, indicates that the niobate nanosheets adsorbing H_2TMPyP are homogeneously distributed in the colloid. However, sample **3b**, which was subjected to the concentration–dilution cycle, gives the image where the fluorescent area is heterogeneously distributed in the view. This image showed the segregation of the niobate nanosheets in

the colloid after the concentration treatment.

TEM observations also indicate that the morphology of each niobate nanosheet is modified upon concentration of the colloid. An image of the nanosheets recovered from the concentrated colloid **3a** is shown in Fig. 2b, and indicates many crumpled and aggregated particles, in contrast with the unconcentrated sample **1** (Fig. 2a), which gives unwrinkled flakes. This result suggests that the nanosheets are deformed and aggregated upon concentration of the colloids. Although the TEM observations are ambiguous because aggregation of the nanosheets could occur during preparation of the specimens upon drying the colloid, the result is consistent with that of fluorescence microscopy indicating the nanosheet segregation upon concentration.

The concentration history of the niobate nanosheet colloids is also reflected by the settling behavior. The dispersed nanosheets gradually settle out with gravity upon standing for long time. We examined the height of the nanosheets settled out in a vessel after 3 weeks of standing the colloid. As shown in Fig. 2, the nanosheets are piled up higher in sample **3b**, which was subjected to the concentration–dilution cycle, than in unconcentrated sample **1**. This result is in agreement with those of microscopic observations if we assume that the niobate nanosheets are aggregated during concentration, which enhances the settlement, although the height of the sediment is a quantitatively inaccurate measure of the amount of settled nanosheets.

Electrolyte Effect on the Spectral Behavior. Addition of electrolytes to the nanosheet colloid altered the visible spectrum of the adsorbed porphyrin similar to the concentration. As shown in Fig. 4h, absorption spectrum of sample **5**, which was prepared by adding KCl to the unconcentrated colloid, is characterized by the split Soret band of H_2TMPyP , being almost the same as observed for the highly concentrated colloid. Hence, the spectroscopically detected modification of the colloid after the concentration by heating is related to enrichment of the electrolytes in the colloid.

Concentration and electrolyte effects were also reflected in the fluorescence spectra. Figure 6 shows the steady-state fluorescence spectra of an aqueous H_2TMPyP solution and the nanosheet colloid samples. The colloid samples exhibited spectra characterized by two resolved emission bands at round 660 and 715 nm, in contrast to aqueous solutions which show an unresolved band. Intensity of the high-energy band relative to the low-energy one is somewhat larger for the concentrated and electrolyte-added colloids (samples **3a** and **5**, Figs. 6c and 6e) that exhibit a split Soret absorption band than that for the colloids characterized by the single Soret absorption (samples **1** and **4**, Figs. 6b and 6d).

Discussion

Our results concern colloidal behavior of the exfoliated niobate nanosheets with macroscopic and molecular-level hierarchies. Concentration of the colloids irreversibly caused aggregation and crumpling of the dispersed nanosheets, as shown by fluorescence microscopy and TEM, which is linked to the modification of microenvironments around H_2TMPyP molecules adsorbed on the nanosheets. The morphological transformation of the nanosheets at macroscopic level is related to the

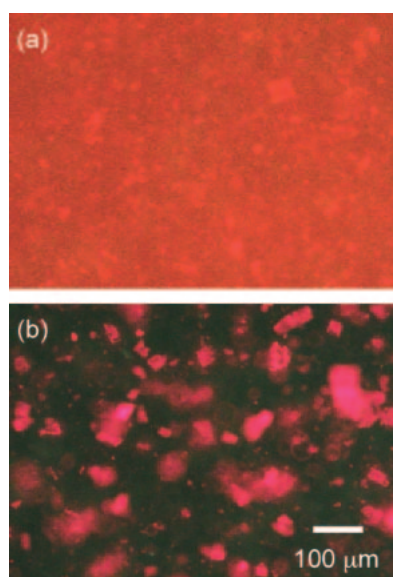


Fig. 5. Fluorescence microscope images of (a) sample **1** (starting unconcentrated nanosheet colloid) and (b) sample **3a** (highly concentrated and re-diluted nanosheet colloid).

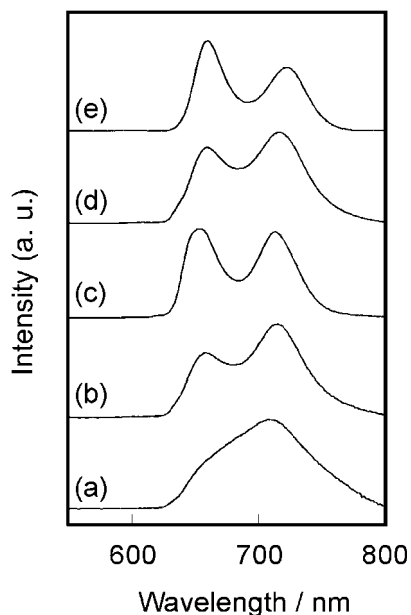


Fig. 6. Fluorescence spectra of (a) H_2TMPyP aqueous solution ($1.3 \times 10^{-5} \text{ mol dm}^{-3}$), (b) sample **1** (starting unconcentrated nanosheet colloid), (c) sample **3a** (highly concentrated nanosheet colloid), (d) sample **4** (nanosheet colloid where H_2TMPyP was added after concentration), and (e) sample **5** (electrolyte-added nanosheet colloid).

bulk properties of the colloid as evidenced by the settling behavior. On the other hand, the porphyrin species adsorbed on the dispersed nanosheets is regarded as a spectroscopic probe of the colloidal properties at the microscopic level.

Effect of the concentration treatment is explained by an increase in the concentration of the electrolyte in the solvent, as indicated by the resemblance of the spectra of the concentrated (samples **2** and **3**) and electrolyte-added (sample **4**) colloids. The unconcentrated nanosheet colloid (sample **1**) contains a certain amount of electrolytes, which are H_2TMPyP cations, propylammonium cations (utilized to exfoliate the niobate and possibly remaining after washing the colloid), and their counter anions. These ionic species are concentrated together with the nanosheets by heating the colloid. Hence, the nanosheets aggregate through screening the electrical double layer at the nanosheet surface; the crumpling and folding of nanosheets observed in the TEM image can be interpreted as the results of intra-particle aggregation. We presume that the H_2TMPyP molecules play an important role in aggregation. The tetravalent porphyrin cations should be strongly attracted by the negatively charged niobate layers. Thus, they should behave as cores around which the nanosheets are irreversibly aggregated, which would explain the “memorization” of concentration history after the concentration–dilution process.

The spectroscopic behavior of H_2TMPyP indicates that the dye molecules in the concentrated nanosheet colloids are present in microenvironments different from those of the unconcentrated colloid. Since the colloid to which H_2TMPyP was added after the concentration (sample **4**) does not show spectral changes, the microenvironments are not on the external surfaces exposed to the solvent but closed spaces which are inaccessible to the porphyrin molecules. Hence, we suppose that

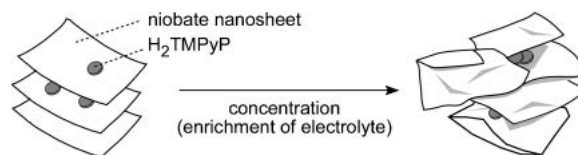


Fig. 7. Schematic illustration of the microscopic event which the niobate nanosheets experience. The colloiddally dispersed nanosheets crumple and partly aggregate upon concentration. H_2TMPyP molecules that are electrostatically bound to the nanosheets are confined in the internal microvoids formed by wrinkling the nanosheets.

the niobate nanosheets aggregated around the H_2TMPyP molecules form internal microvoids to confine the porphyrin molecules. A recent small-angle neutron scattering study of a concentrated liquid crystalline niobate nanosheet colloid ($1.4 \times 10^{-1} \text{ mol dm}^{-3}$) has suggested that the colloiddally dispersed nanosheets are not flat but undulated to form water pockets inside the liquid crystalline domains.²⁴ If the undulated nanosheets adhere to each other through screening of the electrical double layer, the water pockets can transform to closed microvoids. Figure 7 shows a schematic model of the morphological transformation of nanosheets upon concentration.

The split Soret absorption of H_2TMPyP suggests conformational distortion of the porphyrin molecules confined in the aggregated niobate nanosheets. H_2TMPyP molecules intercalated in layered clay minerals have been reported to exhibit split Soret absorptions due to both distortion of the porphyrin ring into a non-planar conformation and modification of the dihedral angle between the porphyrin ring and methylpyridinium substituents.¹⁶ A similar situation involving H_2TMPyP molecules can be the case in our system, and the fluorescence spectra supports such a consideration. Vergeldt et al. have reported that the fluorescence behavior of H_2TMPyP is related to rotational freedom of the methylpyridinium substituents.²⁵ Our results (Fig. 6) showing a variation in the relative intensity of the two emission bands of H_2TMPyP adsorbed on the niobate nanosheets can be explained by differences in the rotational freedom due to the aggregation of the nanosheets. On the other hand, exciton coupling can also account for the splitting of the Soret absorption band, as has been observed for polymeric porphyrin species.^{13,26} However, the density of H_2TMPyP molecules on the niobate nanosheets is low as mentioned above. Thus, exciton coupling, typically facilitated by stacking of porphyrin rings in face-to-face arrangements should not have a large contribution to the spectroscopic behavior of H_2TMPyP in our system, although the porphyrin molecules could become close through the aggregation of nanosheets.

Conclusion

The present study showed that the cationic H_2TMPyP molecules are tightly bound to the anionic hexaniobate nanosheets, and microenvironments around the nanosheets were spectroscopically observed. The spectroscopic behavior of porphyrin indicated irreversible modification of the dispersed state of the niobate nanosheet colloid at molecular level upon concentrating the colloid. Fluorescence microscopy and TEM observations showed that the spectroscopic behavior is related to not only the molecular-level microenvironments of the nano-

sheets but also their macroscopic status, indicating that the porphyrin works as a spectroscopic probe of the colloid. On the other hand, the results also serve as a "caution" about the handling of colloidal dispersions of exfoliated nanosheets, because the nanosheets can be modified with routine treatments like concentration. Such flexibility in the microenvironments is, however, a characteristic aspect of the nanosheet colloids as "soft matrices" for photofunctional molecules.

This work was supported by a Grant-in-Aid for Scientific Research (No. 16350107) from the Ministry of Education, Culture, Sports, Science and Technology, Japan, and a Research Support by Hosokawa Powder Technology Foundation.

References

- 1 a) A. J. Jacobson, in *Comprehensive Supramolecular Chemistry*, ed. by G. Alberti, T. Bein, Pergamon, New York, **1996**, Vol. 7, p. 315. b) E. R. Kleinfeld, G. S. Ferguson, *Science* **1994**, *265*, 370.
- 2 S. W. Keller, H.-N. Kim, T. E. Mallouk, *J. Am. Chem. Soc.* **1994**, *116*, 8817.
- 3 K. Domen, J. N. Kondo, M. Hara, T. Takata, *Bull. Chem. Soc. Jpn.* **2000**, *73*, 1307.
- 4 M. M. J. Treacy, S. B. Rice, A. J. Jacobson, J. T. Lewandowski, *Chem. Mater.* **1990**, *2*, 279.
- 5 M. Fang, C. H. Kim, G. B. Saupe, H.-N. Kim, C. C. Waraksa, T. Miwa, A. Fujishima, T. E. Mallouk, *Chem. Mater.* **1999**, *11*, 1526.
- 6 R. Abe, K. Shinohara, A. Tanaka, M. Hara, J. N. Kondo, K. Domen, *Chem. Mater.* **1997**, *9*, 2179.
- 7 a) T. Sasaki, M. Watanabe, H. Hashizume, H. Yamada, H. Nakazawa, *Chem. Commun.* **1996**, 229. b) T. Sasaki, M. Watanabe, H. Hashizume, H. Yamada, H. Nakazawa, *J. Am. Chem. Soc.* **1996**, *118*, 8329.
- 8 D. M. Kaschak, J. T. Lean, C. C. Waraksa, G. B. Saupe, H. Usami, T. E. Mallouk, *J. Am. Chem. Soc.* **1999**, *121*, 3435.
- 9 W. Sugimoto, O. Terabayashi, Y. Murakami, Y. Takasu, *J. Mater. Chem.* **2002**, *12*, 3814.
- 10 T. Nakato, N. Miyamoto, A. Harada, *Chem. Commun.* **2004**, 78.
- 11 H. van Olphen, *Clay Colloid Chemistry*, 2nd ed., Krieger, Malabar, **1991**.
- 12 a) A. Mamedov, J. Ostrander, F. Aliev, N. A. Kotov, *Langmuir* **2000**, *16*, 3941. b) M. Eckle, G. Decher, *Nano Lett.* **2001**, *1*, 45. c) Z. Tang, N. A. Kotov, S. Magonov, B. Ozturk, *Nat. Mater.* **2003**, *2*, 413. d) D. L. Feldheim, K. C. Graber, M. J. Natan, T. E. Mallouk, *J. Am. Chem. Soc.* **1996**, *118*, 7640. e) T. Takei, Y. Kobayashi, H. Hata, Y. Yonesaki, N. Kumada, N. Kinomura, T. E. Mallouk, *J. Am. Chem. Soc.* **2006**, *128*, 16634. f) Z. Liu, R. Ma, M. Osada, N. Iyi, Y. Ebina, K. Takada, T. Sasaki, *J. Am. Chem. Soc.* **2006**, *128*, 4872. g) L. Wang, Y. Omomo, N. Sakai, K. Fukuda, I. Nakai, Y. Ebina, K. Takada, M. Watanabe, T. Sasaki, *Chem. Mater.* **2003**, *15*, 2873. h) N. A. Kotov, I. Dékány, J. H. Fendler, *Adv. Mater.* **1996**, *8*, 637.
- 13 N. Aratani, A. Osuka, H. S. Cho, D. Kim, *J. Photochem. Photobiol., C* **2002**, *3*, 25.
- 14 Y. Kobuke, K. Ogawa, *Bull. Chem. Soc. Jpn.* **2003**, *76*, 689.
- 15 a) V. G. Kuykendall, J. K. Thomas, *Langmuir* **1990**, *6*, 1350. b) T. Nakato, Y. Iwata, K. Kuroda, M. Kaneko, C. Kato, *J. Chem. Soc., Dalton Trans.* **1993**, 1405. c) Z. Chernia, D. Gill, *Langmuir* **1999**, *15*, 1625. d) M. A. Bizeto, D. L. A. De Faria, V. R. L. Constantino, *J. Mater. Sci. Lett.* **1999**, *18*, 643. e) S. Takagi, T. Shimada, T. Yui, H. Inoue, *Chem. Lett.* **2001**, 128. f) Z. Tong, T. Shichi, Y. Kasuga, K. Takagi, *Chem. Lett.* **2002**, 1206. g) M. Eguchi, S. Takagi, H. Tachibana, H. Inoue, *J. Phys. Chem. Solids* **2004**, *65*, 403. h) M. Eguchi, S. Takagi, H. Inoue, *Chem. Lett.* **2006**, 35, 14.
- 16 a) P. M. Dias, D. L. A. De Faria, V. R. L. Constantino, *J. Inclusion Phenom.* **2000**, *38*, 251. b) P. M. Dias, D. L. A. De Faria, V. R. L. Constantino, *Clays Clay Miner.* **2005**, *53*, 361.
- 17 S. Takagi, T. Shimada, M. Eguchi, T. Yui, H. Yoshida, D. A. Tryk, H. Inoue, *Langmuir* **2002**, *18*, 2265.
- 18 N. Miyamoto, T. Nakato, *J. Phys. Chem. B* **2004**, *108*, 6152.
- 19 N. Miyamoto, H. Yamamoto, R. Kaito, K. Kuroda, *Chem. Commun.* **2002**, 2378.
- 20 K. Nassau, J. W. Shiever, J. L. Bernstein, *J. Electrochem. Soc.* **1969**, *116*, 348.
- 21 N. Miyamoto, T. Nakato, *Adv. Mater.* **2002**, *14*, 1267.
- 22 a) J.-C. P. Gabriel, P. Davidson, *Top. Curr. Chem.* **2003**, *226*, 119. b) L. Onsager, *Ann. N.Y. Acad. Sci.* **1949**, *51*, 627.
- 23 A unit cell of $\text{K}_4\text{Nb}_6\text{O}_{17} \cdot 3\text{H}_2\text{O}$ ($Z = 4$) consists of 4 niobate layers and 16 K^+ ions.²⁰ The surface area of the niobate layers is calculated based on the lattice constants²⁰ to be $a \times c \times 8$ (front and back surfaces of 4 layers) = $0.758 \text{ nm} \times 0.640 \text{ nm} \times 8 = 3.88 \text{ nm}^2$. Since the reaction of $\text{K}_4\text{Nb}_6\text{O}_{17}$ with propylammonium ions gives bilayer-type nanosheets,¹⁹ 2 inter-layer spaces per unit cell should be exposed to the porphyrin molecules. Thus, exfoliated $\text{K}_4\text{Nb}_6\text{O}_{17}$ gives $3.88/2 = 1.94 \text{ nm}^2$ of the layer surface exposed to H_2TMPyP molecules per a unit cell (=4 niobate molecules). Since the molar ratio of $\text{H}_2\text{TMPyP}/\text{Nb}_6\text{O}_{17}$ is 5×10^{-3} , each porphyrin molecule occupies $1.94/4/5 \times 10^{-3} = 97 \text{ nm}^2$ of nanosheet surface on average.
- 24 D. Yamaguchi, N. Miyamoto, S. Koizumi, T. Nakato, T. Hashimoto, *J. Appl. Crystallogr.* **2007**, *40*, s101.
- 25 F. J. Vergeldt, R. B. Koehorst, A. van Hoek, T. J. Schaafsma, *J. Phys. Chem.* **1995**, *99*, 4397.
- 26 M. Fujitsuka, A. Okada, S. Tojo, F. Takei, K. Onitsuka, S. Takahashi, T. Majima, *J. Phys. Chem. B* **2004**, *108*, 11935.